

Chemical State Analysis by Auger Microprobe with Hemispherical Energy Analyzer

Y. Sakai, M. Kudo, T. Yamada, N. Ikeo and Y. Nagasawa

JEOL LTD, 3-1-2 Musashino, Akishima, Tokyo 196-8558 Japan

(Received October 5 1998; accepted January 13 1999)

Auger microprobe equipped with a hemispherical energy analyzer (HSA) has been developed for measurements of high energy resolution Auger spectra. HSA is usually used in X-Ray photoelectron spectroscopy with a high energy resolution. In this paper, the technical improvements of new input lens and multi-channel detector system combined with HSA are presented with applications of Auger chemical state analysis.

1. Introduction

Auger electron microprobe has been used as a powerful tool for micro-analysis on the surface. To improve a performance of the Auger microprobe, JAMP-7800F was equipped with a ZrO/W Schottky field emission gun, a newly designed objective lens and an image drift compensation system [1]. Furthermore, a hemispherical analyzer (HSA) was installed with this instrument as an electron energy analyzer [2]. In general, HSA or the concentric hemispherical analyzer (CHA) is usually used in X-Ray photoelectron spectroscopy (XPS), because of the high energy resolution. By combination of HSA with an Auger electron microscope, Auger chemical state analysis was possible in micro-area. In this paper, the technical improvement of a new input lens system and a multi-channel detection system combined with HSA for Auger electron micro-analysis are presented with applications of Auger chemical state analysis.

2. Experimental

To use the HSA in Auger electron spectroscopy (AES), a new HSA detection system was developed with a new input lens system. A schematic drawing of the HSA detection system is shown in Figure 1. This system consists of two new functions, i.e., the input lens system and the multi-channel detection system.

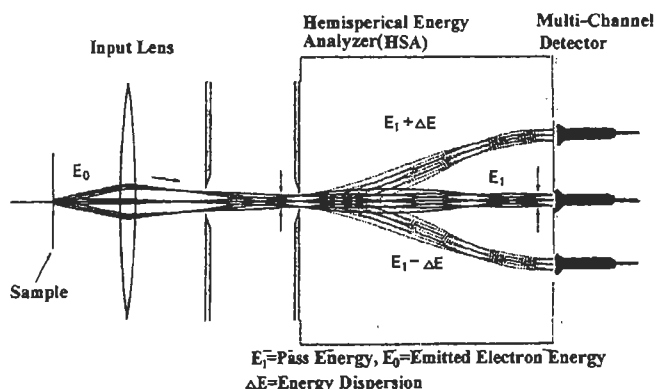


Fig. 1 HSA detection system with multiple detector: The system consists in input lens with hemispherical analyzer and multi-channel detector.

A sensitivity of the Auger detection system depends on the design of the input lens system and the multi-channel detection system installed with HSA.

2-1. Input lens system for HSA

Electrons emitted from a specimen by electron excitation are decelerated and focused onto the entrance plane of HSA by an action of the input lens system. The energy of electrons is filtered by HSA. The electrons energetically dispersed at the output position of HSA are detected by several multi-channel detectors. The design concept of the input lens system used in XPS is applied to AES. For the conventional XPS, the analyzer is designed to detect the signals distributed uniformly over the area of several mm^2 . While, in AES, a signal source is limited in a very small area. Thus, the design of the input lens system has been carried out by computer simulation.

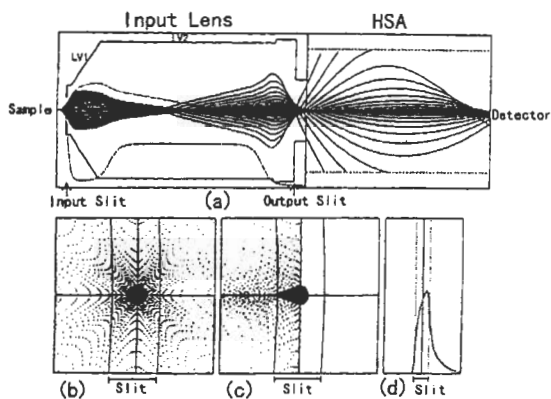


Fig. 2 Trajectories in input lens and HAS by computer simulation. (a) The emission angles are from $\pm 2^\circ$ to $\pm 12^\circ$ with 2° steps. The calculating conditions is emitted electron energy (E_0)=885 eV, pass energy (E_1)=30 eV, Lens 1 bias voltage (LV1)=-800 V and Lens 2 bias voltage (LV2)=-27 eV, (b) Spot diagram at HSA input slit position, (c) Spot diagram at HSA output slit position, (d) Line shape at HSA output slit position

For the point source, the trajectories of electrons in the input lens and the HSA are shown in Figure 2. The electrons are focused onto the input slit of HSA under a high magnification. The aberration of the input lens system affects to the beam shape, and lowers the detection efficiency. The shorter working distance of the input lens lowers the aberration, and leads to increase the detection solid angle. Figure 3 shows the spherical aberration coefficient as a function of retarding potential ratio, E_0/E_1 [3]. In the constant retarding ratio (CRR) mode, the retarding ratio is set from 0.2 to 50 and the aberration coefficient is about 1000 mm compared to 3000 mm of that of the XPS input lens. This fact contributes to the increasing of the sensitivity.

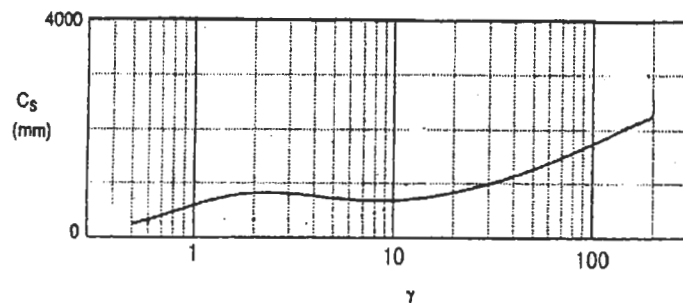


Fig. 3 Spherical aberration coefficient(C_s) as function of retarding potential ratio $\gamma=(E_0/E_1)$.

2-2. Multi-channel detection system

HSA is an energy dispersive analyzer and the electrons passed through between electrostatic deflectors focus at the output plane of HSA by proportion to the electron energy. The multi-channel detectors placed at the dispersion position on the output plane detect all available signals for a spectrum. The sensitivity increases proportional to the number of detectors introduced. There are two analyzing modes in the use of HSA.

In constant retarding ratio (CRR) or constant relative resolution mode, the electrons are decelerated by a constant factor or ratio, from their initial kinetic energies. Clearly this mode operates at the constant relative resolution ($\Delta E/E_0$). On the other hand, in constant analyzing energy (CAE) or constant absolute resolution (CAR) mode used in XPS, the electrons are decelerated to a constant pass energy E_1 and it is obvious that the mode is that of constant absolute resolution (ΔE). The channeltrons detect the electrons at the constant resolution for sweep of retarding potential. In CRR mode used in AES, the pass energy E_1 changes with the retarding potential and the energy resolution at the output plane changes also with the retarding potential. The channeltrons detect dispersed electrons at the different positions. The new detection system consisting of several channeltrons at the dispersion plane detects the dispersed electrons and corrects the energy dispersion. Data acquired from each channel through the retarding potential sweep are consolidated into single spectrum. This energy dispersion correction method for the data acquisition allows the HSA in the use of AES.

3. Applications

3-1. High energy resolution spectra

The energy resolution changes with the retarding voltage applied to the HSA. The relative energy resolution ($\Delta E/E_0$) from 0.03 to 0.8% is obtained. Figure 4 shows the Si-KLL Auger spectra at different energy resolutions of 0.5%, 0.35% and 0.15%.

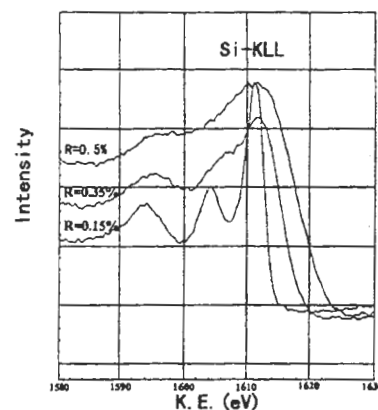


Fig. 4 Si-KLL Auger spectra with 0.15%, 0.35% and 0.5% of energy resolution ($\Delta E/E_0$)

3-2. Auger chemical state analysis

The chemical state of Si is measured for an IC pattern which consists of Si, SiO₂ and Si₃N₄. Figure 5 shows Auger electron spectra from the IC pattern at three points where element and compound names are indicated on the secondary electron image (SEI) of Fig. 6(a).

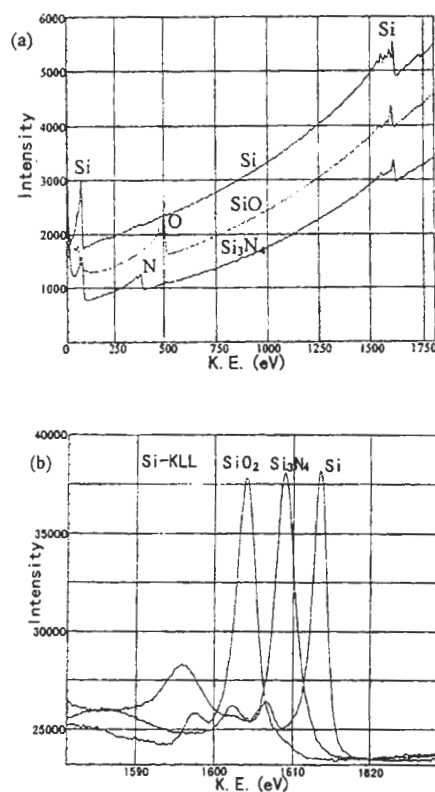


Fig. 5 Auger chemical state spectra of Si, SiO₂ and Si₃N₄. (a) is wide spectra with energy resolution 0.5%. (b) is energy spectra with high energy resolution 0.15%.

Figure 5 shows the chemical state spectra measured at the high energy resolution of 0.15%. The energy shifts of Si-KLL for SiO_2 and Si_3N_4 are 9.4 and 4.4 eV. The peak position and the change of shape depends on chemical bonding.

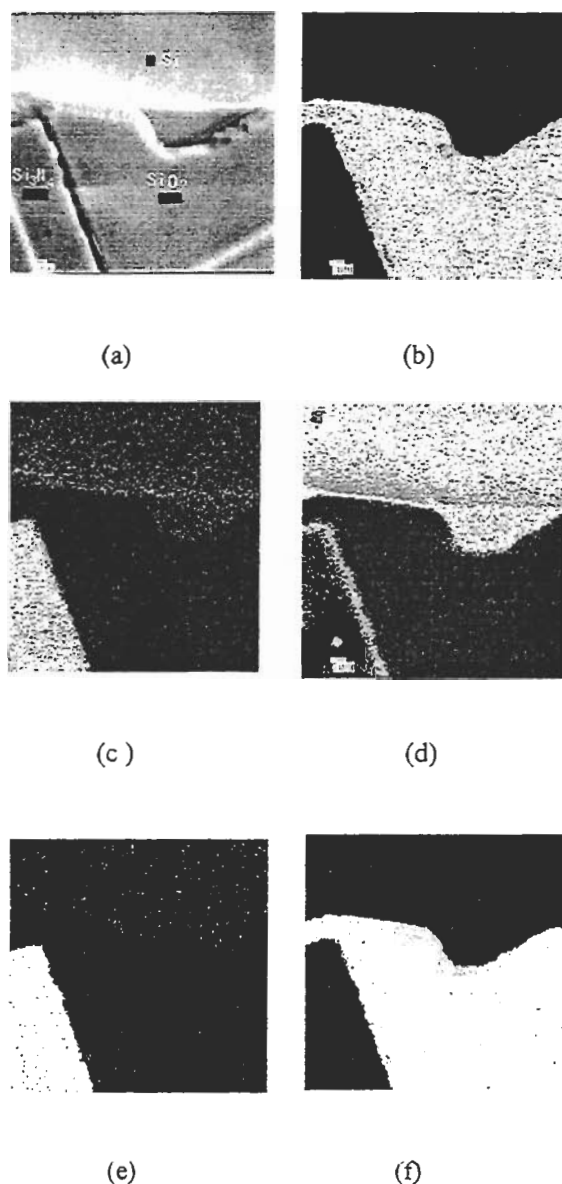


Fig. 6 Secondary electron images (SEI) and Auger images of integrated circuit. (a) is SEI of IC. The analyzing points of Fig.5 are corresponded to the element name position in (a). (b), (c), (d) are Auger chemical images of SiO_2 , Si_3N_4 and Si, and (e), (f) are Auger images of N-KLL and O-KLL respectively.

Images of chemical state mapping are shown in Figure 6. In Fig. 6, (b), (c) and (d) are Auger electron images of Si-KLL for SiO_2 , Si_3N_4 , and Si, and (e) and (f) are Auger images of N-KLL and O-KLL, respectively. The distributions of Si nitride and Si oxide are clearly observed from the chemical shift of Si-KLL.

4. Summary

The HSA is applied to Auger electron spectroscopy with decreasing aberrations for the input lens system and improving the detection system. By this technique, the Auger electron microscope with HSA allows Auger chemical state analysis in the microscopic dimension. The typical applications to the integrated circuit show that Auger chemical state analysis becomes possible on spectroscopy and mapping in the microscopic dimension.

References

- [1] T. Yamada, M. Kudo, Y. Ando, T. Sekine and Y. Sakai, *Applied Surface Science* 100/101(1996) 287-291.
- [2] T. Sekine, N. Ikee and Y. Nagasawa, *Applied Surface Science* 100/101(1996) 30-35.
- [3] M. Kato. Doctor Thesis (Tokyo univ.) (1997).